NJC

Accepted Manuscript

This is an *Accepted Manuscript*, which has been through the Royal Society of Chemistry peer review process and has been accepted for publication.

Accepted Manuscripts are published online shortly after acceptance, before technical editing, formatting and proof reading. Using this free service, authors can make their results available to the community, in citable form, before we publish the edited article. We will replace this *Accepted Manuscript* with the edited and formatted *Advance Article* as soon as it is available.

You can find more information about *Accepted Manuscripts* in the Information for Authors.

Please note that technical editing may introduce minor changes to the text and/or graphics, which may alter content. The journal's standard Terms & Conditions and the Ethical guidelines still apply. In no event shall the Royal Society of Chemistry be held responsible for any errors or omissions in this *Accepted Manuscript* or any consequences arising from the use of any information it contains.

ROYAL SOCIETY OF CHEMISTRY

www.rsc.org/njc

Carbonized non-woven fabrics films as adsorbing interlayers to enhance electrochemical performance of lithium sulfur batteries

Zhaoxia Cao,[a,b,c] Chao Ma,[a,b,c] Yanhong Yin,[a,b,c] Jun Zhang,[a,b,c] Yanmin Ding,[a,b,c] Mengjiao Shi, [a,b,c] Shuting Yang,*[a,b,c]

a. School of Chemistry and Chemical Engineering, Henan Normal University, Xinxiang Henan 453007, P. R. China

b. National and Local Joint Engineering Laboratory of Motive Power and Key Materials, Xinxiang Henan 453007, P. R. China

c. Collaborative Innovation Center of Henan Province for Green Motive Power and Key Materials, Henan Normal University, Xinxiang Henan 453007, P. R. China

*Corresponding author: Shuting Yang

E-mail address: shutingyang@foxmail.com

Tel.: (+86)-373-3326439, Fax: (+86)-373-3326439

Abstract

Lithium Sulfur (Li-S) batteries with an effective adsorbing interlayer, high capacity and long cycle life have been fabricated with a simple method by placing an interlayer between the sulfur cathode and the separator. The interlayer with optimized porosity, electrolyte uptake and electrical conductivity can facilitate the use of pure sulfur (with a sulfur content of 70%) as a highly reversible cathode, which was made of the carbonized non-woven fabrics (*Mind Act Upon Mind*™ Skincare Wipes) modified with Ketjen Black. A high capacity of 1486 mA h g^{-1} at a rate of 0.1 C (1 C=1675 mA g^{-1}) in the first cycle was obtained, and the reversible capacity remains retained high up to 858 mA h g^{-1} even after 100 cycles.

Key words: Interlayer, cathode, structure designing, lithium–sulfur battery, cycling stability

1. Introduction

Lithium-sulfur (Li-S) battery is presently one of the most promising systems for a future generation of Lithium rechargeable batteries. The main advantages such as the high theoretical capacity (1675 mA h g^{-1}) and high energy density (2600 Wh kg^{-1}) have aroused considerable interests [1-5]. Moreover, the elemental sulfur is abundant, low-costly and environment friendly.

However, the low utilization and poor cycling life of the sulfur cathode become major problems of lithium sulfur batteries for practical application which mainly originates from the dissolution and shuttle effect of lithium polysulfides as intermediate generated products during the electrochemical process and so on [6]. In addition, both sulfur and its insoluble discharge products (*i.e.*, Li_2S/Li_2S_2) are electronic and ionic insulators, thus bring out the poor reaction kinetics.

Over the past decades, Much efforts were made to integrate sulfur with carbonaceous materials to raise the practical discharge capacity such as micro/mesoporous carbon [7-9], carbon nanotubes [10-13], carbon spheres [14, 15], graphene oxide [16, 17], porous/hollow carbon nanofibers [18] and ordered mesoporous carbon [19, 20] with sulfur content no more than 70% in most cases. However, carbonaceous materials alone cannot effectively prevent the diffusion of the polysulfides and the shuttle effect.

Thus, an additional barrier layer was frequently sandwiched between S and Li electrodes to further block the diffusion of polysulfides. The barrier layer can be directly attached to the surface of the sulfur cathode, or be inserted as an interlayer between the separator and conventional sulfur cathode. Microporous carbon paper, interwoven carbon nanotubes, biomaterials, rGO films have been inserted as interlayer[21-28]. The soluble polysulfides can be effectively localized within the cathode region. Moreover, the carbon interlayer can reduce the polarization of the cell significantly. The cycle performance is enhanced self-evidently with the simple strategy.

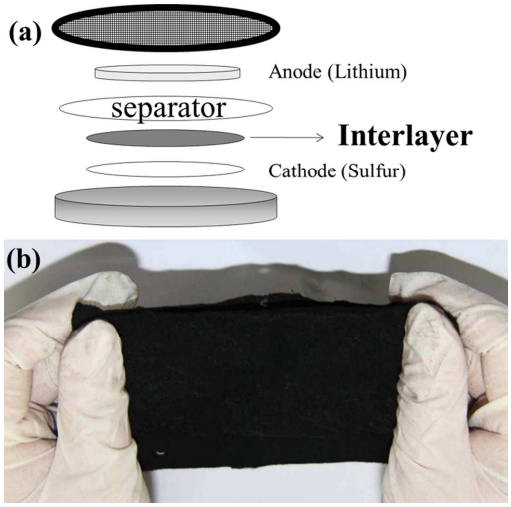

Fig. 1 Schematic of Li-S battery with interlayer

In this study, a carbonized non-woven fabrics film modified with Ketjen Black（CF）was used as the adsorbing interlayer between the pure sulfur cathode and the separator in Li-S batteries, which facilitates the use of pure sulfur with a sulfur content of 70% as a highly reversible

cathode (Fig. 1a). The film possesses good mechanical strength (Fig. 1b), excellent conductivity, large electrolyte uptake and adjustable porosity. Some advantages were provided by the interlayer: the interwoven fibre assisting the electron transport and enhancing the cathode conductivity, the controllable porosity and large electrolyte uptake ensuring an excellent electrolyte immersion/penetration upon cell cycling and suppressing the migration of polysulfides. Therefore, cells with the interlay achieve high discharge capacity and excellent cyclability.

2. Experimental

2.1 Material preparation

The non-woven fabrics (*Mind Act Upon Mind*™ Skincare Wipes) were soaked in alcohol for 12 h, cleaned with deionized water, and then dried at room temperature. The filler was made by mixing the Ketjen Black (EC600JD) and polyvinylidene fluoride (PVDF) (80:20 by weight) with N-methyl-2-pyrrolidine (NMP) as solvent in an agate mortar. After mixing homogeneously, the slurry was coated onto non-woven fabrics using a glass rod. The pre-fabrics were dried for 10 h in drying oven, and then were calcined in a box-type furnace under a following N_2 atmosphere for 6 h with a heating rate of 5 °C min^{-1}. The samples was named as CF-1 (untreated), CF-2 (300 °C), CF-3 (350 °C) and CF-4 (400 °C) according the heat treatment temperature, respectively. When

the temperature reaches 450 °C, The fabrics have break down, leading to poor mechanical strength.

2.2 Material Characterization

The morphology of samples was observed using a scanning electron microscopy (SEM, HITACHI, TM3000) and energy dispersive X-ray spectrometer (EDS). N_2 adsorption-desorption isotherms (BET, Tristar-Ⅱ, Micromeritics) were measured to elucidate the BET surface area, pore volume and pore distribution.

The porosity and electrolyte uptake of samples were measured by traditional solvent absorptivity test. The dry film were immersed in 1 M Li-TFSI dissolved in a 2 : 1 (v/v) mixture of DME and DOL electrolyte for 24 hours at room temperature. After quickly wiping out the surface electrolyte of the membranes, the weight of membrane was measured. The electrolyte uptake of the membranes can be calculated based on the weight difference between the dried and soaked film. Electrical conductivity was tested by electrochemical impedance spectroscopy (EIS) with CHI660B electrochemical workstation.

2.3 Electrochemical measurements

For electrochemical evaluation, CR2016 coin cells were fabricated in an argon filled glove box. The working electrode was made by mixing the sublimed sulfur, Super P and CMC with distilled water as solvent in

a weight ratio of 70:20:10. The mass loading of sulfur in the electrode is 2mg cm^{-2}.The separator is a polypropylene membrane with micropores (Celgard 2400). Lithium metal is used as anode electrode. As the insertion, a carbonized non-woven fabrics film (cut into circular disc) was placed between the cathode and the separator.

The electrolyte used is 1 M LITFSI in a mixture of Dimethoxyethane (DME) and 1, 3-Dioxolane (DOL) (2:1 volume), including 0.1 M $LiNO_3$ as an electrolyte additive. Galvanostatic charge–discharge experiment data were collected using LAND Cell test system (CT2001A, Wuhan, China). A.C. impedance and cyclic voltammetry (CV) measurements were conducted with a CHI660B electrochemical workstation using fresh cells at open potential. A.C. impedance spectra were measured at 10 mV amplitude with a frequency range from 0.1 Hz to 100 KHz. The CV measurement was performed in the range of 1.2-2.8 V at a scanning rate of 0.05 mV s^{-1}.

3. Results and discussion

Table 1 shows the porosity, electrolyte uptake and electrical conductivity of the as-prepared CFs with or without heat-treatment. Although the porosity decreases slightly from 75% to 69% and 71%, then reaching to maximum of 85% at 400 °C, the electrolyte uptake and electrical conductivity of the CFs increase obviously with raised

heat-treatment temperature. The electrolyte uptake varies from 248%, 299%, 324% to 381%, and electronic conductivity from 2.02 × 10^{-5}, 2.05 × 10^{-5}, 3.56× 10^{-4} to 4.57 × 10^{-4}. The CF-4 shows the highest porosity, electrolyte uptake and electrical conductivity.

Table 1 Physical parameters of the CFs as interlayers

	Carbonization temperature / ℃	Porosity / %	Electrolyte uptake / %	Electrical conductivity / S cm^{-1}
CF-1	-	75	248	2.02 × 10^{-5}
CF-2	300	69	299	2.05 × 10^{-5}
CF-3	350	71	324	3.56 × 10^{-4}
CF-4	400	85	381	4.57 × 10^{-4}

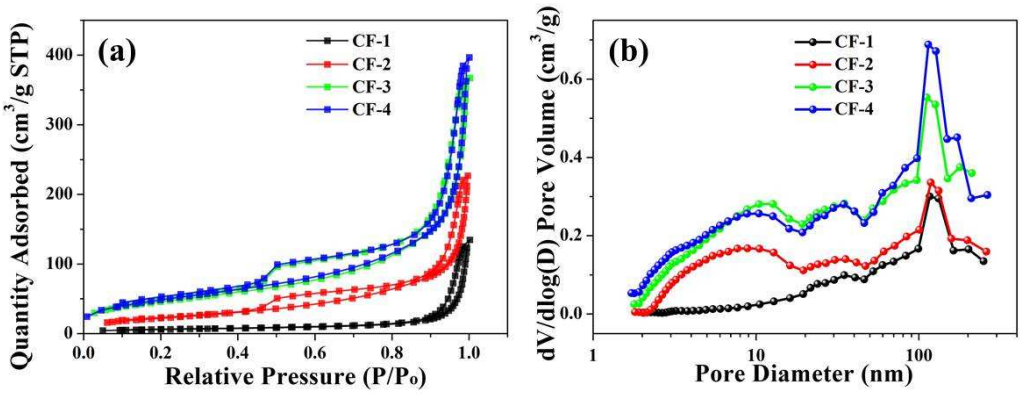

Fig. 2 Nitrogen adsorption/desorption isotherms (a) and pore size distribution plots (b) of CF-1, CF-2, CF-3, CF-4

To elucidate the BET surface area and the porous structure of the CF interlayers, we measured N_2 adsorption-desorption isotherms. The curves can be identified as type IV in the IUPAC classification with typical H4 hysteresis loop as shown in Fig. 2a, which suggests hierarchical porous structure of the CFs. The BET specific surface area

increases with increasing heat-treatment temperature, ranging from 22.45 to 82.58, 164.68 and 174.55 m^2 g^{-1}. The pore size distribution plots (Figure 2b) show that there are newly emerged small pores with diameter of 8 nm as well as an increase of macropores after heat treatment.

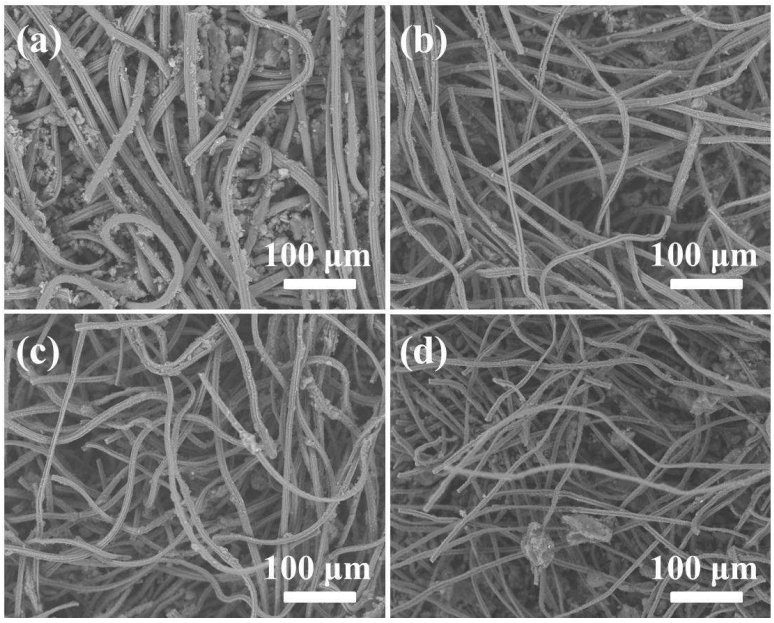

Fig. 3 SEM images of samples with or without heat treatment, (a) CF-1, (b) CF-2, (c) CF-3, (d) CF-4.

Microstructures of the as-prepared films were observed with SEM technique, as shown in Fig. 3. It is clearly seen that the films carbonized at 300 °C, 350 °C and 400 °C maintains its original, are shown in Fig. 2(b-d). As shown in Fig. 3, the fabrics sizes and the gaps between fabrics became small, as increasing the treating temperature. The CF interlayers with a rich porous network structure can absorb more of electrolyte and suppress the migration of polysulfides to anode side

resulting an enhancing electrochemical performance.

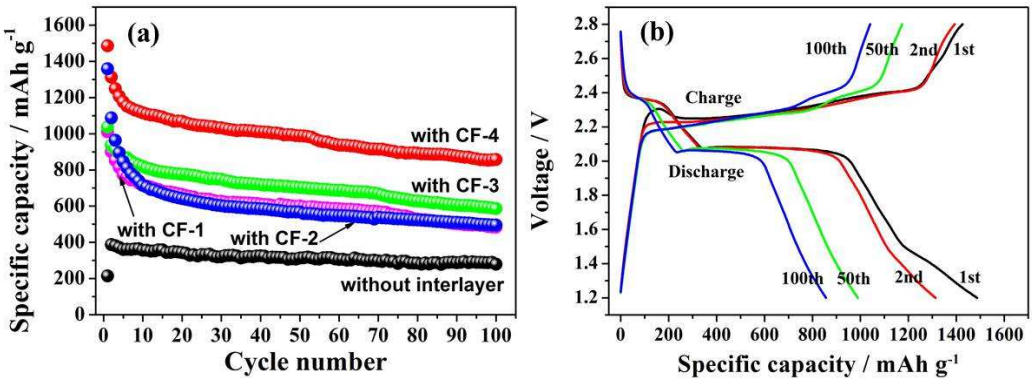

Fig. 4 (a) Cycle performance of the Li-S cells with the CF-1, CF-2, CF-3, CF-4, interlayer and without the interlayer, at a rate of 0.1 C between 1.2 V and 2.8 V at room temperature. (b) Charge-discharge curves in different cycling numbers of the cell with CF-4 at a rate of 0.1 C.

The cycle performance of the Li-S batteries with different interlayers at 0.1 C (1 C=1675 mA g^{-1}) is displayed in Fig. 4a. From the attenuation trend of cycling stability, the batteries with the adsorbing interlayer have obviously excellent performance. The discharging specific capacity is 1011 mA h g^{-1}, 1358.9 mA h g^{-1}, 1037 mA h g^{-1} and 1486 mA h g^{-1}, respectively, at the first cycle. The CF-4 exhibits the best performance with a specific capacity of 858 mA h g^{-1} after 100 cycles. As comparison, the cell without interlayers shows poor performance, indicating that adsorbing interlayers play a positive role. The reasons are that: the porous structure of the CF interlayers as well as high porosity and electrolyte uptake can provide more channels to facilitate lithium ion migration and ensure an excellent electrolyte immersion/penetration as

well as absorb polysulfides at cathode side upon repeated charging-discharging process.

Galvanostatic cycling performance was studied and the typical discharge–charge profiles at the rate of 0.1 C between 1.2 and 2.8 V are presented in Fig. 4b. Two plateaus are presented in the discharge profiles of the cells: a short higher potential plateau at about 2.35 V and the other prolonged lower potential plateau at about 2.05 V. The 2.35 V plateau is ascribed to the transformation from sulfur to the higher-order lithium polysulfides, which are soluble in the liquid electrolyte. Furthermore, at the lower plateau potential the polysulfides react with lithium ions and form Li_2S. The decrease in capacity within the first few cycles could be due to the redistribution of sulfur and the irreversible dissolution of polysulfides into electrolyte. The following enhanced cycle performance should be attributed to the powerful adsorption properties of interlayer which suppress the migration of polysulfides.

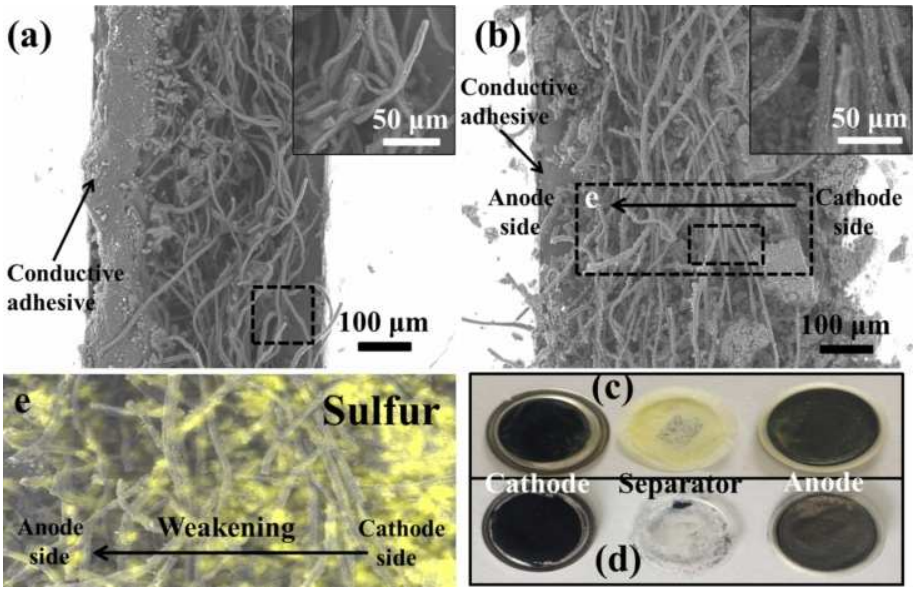

Fig. 5 SEM images of CF-4 cross-section: (a) before cycle, (b) after 100 cycles. Digital photograph of the detachment Li-S cells: (c) without interlayer, (d) with CF-4. (e) The elemental mapping of sulfur of CF-4 after testing.

To reveal the effect of the CF interlayer in suppressing the transition of polysulfides, the SEM images of the cross-section of CF-4 before and after cycling were shown in Fig. 5. The thickness of interlayer was about 200 μm, equal to reported in reference [25]. The fibers of the layer intricately intertwined with smooth surface (Fig. 5a). And the inset image indicated many small particles were loaded on the fibers after cycling (Fig. 5b). The sulfur elemental mapping results of CF-4 after cycles are depicted in Fig. 5e. From cathode side to anode side, the gradual color bleaching indicates the sulfur content is gradually reduced. The phenomenon proves that the CF-4 could suppress the migration of polysulfides. In order to more clearly observe the function of interlayers,

batteries were disassembled after 100 discharge-charge cycles. Fig. 5c shows the cell without interlayer, obviously there was a lot of yellow substance, probably polysulfides, on the surface of separator, even a small amount on anode side. Fig. 5d shows the cell with CF-4. As shown in Fig. 5d, no visible yellow substance appears on separator or anode, just a little black substance, which may be ketjen black. So, it could be speculated that polysulfides were effectively adsorbed on the CF-4, and almost set on the cathode side in the process of electrochemical.

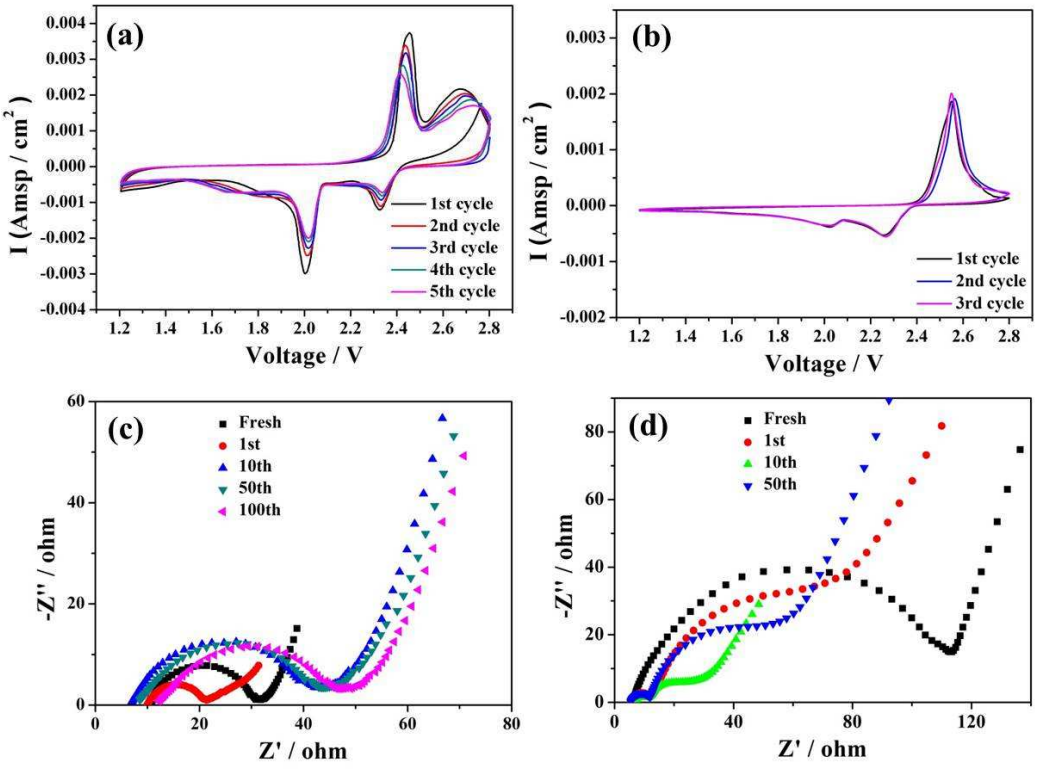

Fig. 6 (a) CV plots and EIS of the Li-S cell with (a) and without (b) CF-4 interlayer. EIS plots of the Li-S cell without (c) and (d) without CF-4 interlayer.

Fig. 6a and 6b shows the cyclic voltammetry (CV) curves of the

cells with and without interlayers. In the cathodic sweep, the CV curves of the two samples display two reduction peaks, related to the reduction of cyclic S_8 to long-chain lithium polysulfides (Li_2S_x, $4 \leq x \leq 8$) and the further reduction of long-chain polysulfides to short-chain lithium polysulfides (Li_2S_x, $1 \leq x \leq 4$) respectivly. In the anodic sweep, only one broad oxidation peak, attributed to the transition of insoluble lithium sulfides to soluble polysulfides and polysulfides to S_8 is observed. The cell with an interlayer shows a more positive reduction potential (2.35V vs 2.28 V), and a more negative oxidation potential (2.45 V vs 2.55 V), indicating improved polarization. Furthermore, mainly complete overlapping of the anodic and cathodic peaks indicates high reversibility after the first three cycles as shown in Fig. 6a. The better electrochemical stability of the cell with the CF-4 is due to the adsorbing of active materials (including polysulfides) and preventing the shuttle mechanism from occurring.

To further verify the improved electrochemical performance, electrochemical impedance spectroscopy (EIS) was carried out for the cells with and without an interlayer at a rate of 0.1 C, from 0.1 Hz to 100 KHz (Fig. 6c and 6d). The EIS spectrum of the cells with interlayers featured a semi-circle in the high to medium frequency region relating to the resistances of charge transfer and a oblique straight line in the low frequency region corresponding to the Li ions diffusion process. The

first cycle is slightly superior to the fresh, after undergoing an electrical activation process. The polysulfides were adsorbed by the interlayer, and diffusion through separators to the anode side was then prevented to some extent. Upon the charge/discharge process, more and more polysulfides were formed and filled in electrolyte. However, When absorption of polysulfides reaches a certain amount of time, resistance becomes stable. The impedance behaviors are similar to each other after 10^{th} cycle to 100^{th} cycles. For comparison, the Nyquist plots of the cells without interlayers after 10 cycles are composed of two semicircles at high frequency and a nearly straight line at low frequency, as shown in Fig. 6d. The two semi-circles in the high to medium frequency region could be ascribled to the resistances of charge transfer and the SEI film, which indicating bad cathode reaction kinetics. It is obvious that the cells with interlayers exhibit a low and stable charge transfer resistance upon cycling, which could be attributed to the enhanced conductivity and the stable structure of the adsorbing interlayer. In addition, this impedance evolution can well match the excellent electrochemical performance with the reversible specific capacity.

The rate capacity performance of the Li-S battery with CF-4 is shown in Fig. 7. During the first 5 cycles, the discharge capacity fades gradually at 0.1 C, further cycling at higher rates shows reversible capacity of 921 mA h g^{-1} (0.2 C, eighth cycle), 795 mA h g^{-1} (0.5 C, 13^{th}

cycle), 677 mA h g^{-1} (1 C, 18th cycle), 520 mA h g^{-1} (2 C, 23th cycle). Specific capacity of the cell can reach 286 mA h g^{-1} (28th cycle) even at the current density is 5 C. After the cell was charge/discharge at different rates, a reversible capacity of 855 mA h g^{-1} could still be retained at 0.1 C after 40 cycles, manifesting an excellent rate performance of the cell. By contrast, the cell without interlayers shows fast capacity fading at the same increasing charge-discharge rate. The excellent rate performance of the cell with interlayers may be attributed to the porous structure in which the sulfur species are distributed and tightly trapped, as well as a reservoir of the liquid electrolyte in which the transfer of lithium ions to active material can be accelerated 85%. The cell with an interlayer of carbonized non-woven fabrics film (CF) modified with Ketjen Black has comparable electrochemical performance to other interlayer synthesized by complicated process, as shown in Table 2.

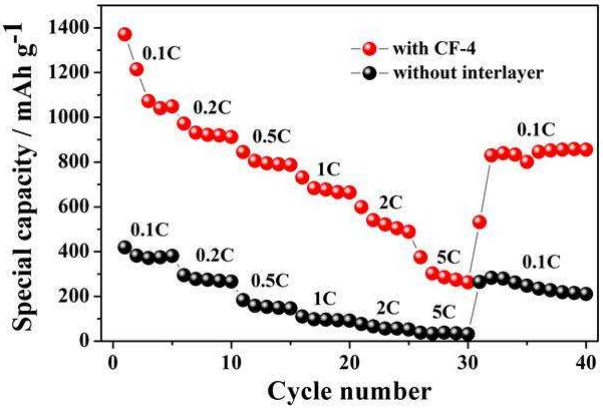

Fig. 7 The rate performance of the cells with and without interlayer.

Table 2 Summary of Li-S battery systems with an interlayer

Samples	Sulfur content	Sulfur loading (mg cm^{-2})	Specific capacity (mA h g^{-1})	Cycles	Ref.
microporous carbon paper	70%	-	1000 at 1 C	100	21
MWCNT interlayer	70%	-	962 at 0.2 C	50	22
rGO interlayer	85%	-	895 at 0.1 C	100	23
Toray carbon paper	60%	-	900 at 0.2 C	50	24
Carbonized Kimwipes	60%	1.1	1086 at 0.1 C	100	25
carbonized leaf	70%	1.3	1013 at 0.1C	100	26
PPy interlayer	65% (80% CMK-8)	1.5	846 at 0.2 C	200	27
pristine filter paper	70%	-	820 at 0.2 C	50	28
			560 at 1 C	50	
interlayer in this work	70%	2	858 at 0.1 C	100	
			677 at 1 C		

4. Conclusions

In conclusion, a simple and effective method is employed to improve electrochemical performance of Li-S batteries with carbonized non-woven fabrics films as interlayers between the sulfur cathode electrode and the separator. The cell with CF-4 (85% porosity, 381% electrolyte uptake and 4.57×10^{-4} S cm^{-1}), shows a highest capacity of 1486 mA h g^{-1} at a rate of 0.1 C in the first cycle and the reversible capacity remains high up to 858 mA h g^{-1} even after 100 cycles. The cells also display a superior performance when cycling at increased rate. The following work is looking for more suitable interlayer materials, optimizing the processing conditions, increasing the sulfur loading to further improve the Li-S battery performance in future.

Acknowledgements

This work was financially supported by Foundation of Henan Educational Committee, the Program for Science & Technology Innovation Talents in Universities of Henan Province; Key Scientific and Technological Project of Henan Province (15A150012) and Key Scientic and Technological Project of Xinxiang (ZG15003).

References

1. G. BrucePeter, A. FreunbergerStefan, J. HardwickLaurence and M. TarasconJean, *Nature materials*, 2012, **11**, 172-172.
2. X. Ji and L. F. Nazar, *Journal of Materials Chemistry*, 2010, **20**, 9821-9826.
3. L. Yin, J. Wang, F. Lin, J. Yang and Y. Nuli, *Energy & Environmental Science*, 2012, **5**, 6966-6972.
4. B. Zhang, X. Qin, G. R. Li and X. P. Gao, *Energy & Environmental Science*, 2010, **3**, 1531-1537.
5. L. Xiao, Y. Cao, J. Xiao, B. Schwenzer, M. H. Engelhard, L. V. Saraf, Z. Nie, G. J. Exarhos and J. Liu, *Advanced materials*, 2012, **24**, 1176-1181.
6. J. Shim, K. A. Striebel and E. J. Cairns, *Journal of The Electrochemical Society*, 2002, **149**, A1321-A1325.
7. S. R. Chen, Y. P. Zhai, G. L. Xu, Y. X. Jiang, D. Y. Zhao, J. T. Li, L. Huang and S.-G. Sun, *Electrochim Acta*, 2011, **56**, 9549-9555.

8. S. R. Zhao, C. M. Li, W. K. Wang, H. Zhang, M. Y. Gao, X. Xiong, A. B. Wang, K. G. Yuan, Y. Q. Huang and F. Wang, *Journal of Materials Chemistry A*, 2013, **1**, 3334-3339.

9. M. R. Wang, H. M. Zhang, Y. N. Zhang, J. Li, F. X. Zhang and W. Hu, *J Solid State Electr*, 2013, **17**, 2243-2250.

10. W. Ahn, K. B. Kim, K. N. Jung, K. H. Shin and C. S. Jin, *Journal of Power Sources*, 2012, **202**, 394-399.

11. M. M. Rao, X. Y. Song and E. J. Cairns, *Journal of Power Sources*, 2012, **205**, 474-478.

12. W. Wei, J. Wang, L. Zhou, J. Yang, B. Schumann and Y. NuLi, *Electrochemistry Communications*, 2011, **13**, 399-402.

13. S. M. AbstractZhang, Q. Zhang, J. Q. Huang, X. F. Liu, W. C. Zhu, M. Q. Zhao, W. Z. Qian and F. Wei, *Part Part Syst Char*, 2013, **30**, 158-165.

14. H. Ye, Y. X. Yin, S. Xin and Y. G. Guo, *Journal of Materials Chemistry A*, 2013, **1**, 6602-6608.

15. M. S. Park, J. S. Yu, K. J. Kim, G. Jeong, J. H. Kim, T. Yim, Y. N. Jo, U. Hwang, S. Kang, T. Woo, H. Kim and Y. J. Kim, *RSC Advances*, 2013, **3**, 11774-11781.

16. J. Z. Wang, L. Lu, M. Choucair, J. A. Stride, X. Xu and H. K. Liu, *Journal of Power Sources*, 2011, **196**, 7030-7034.

17. M. Xiao, M. Huang, S. S. Zeng, D. M. Han, S. J. Wang, L. Y. Sun

and Y. Z. Meng, *Rsc Advances*, 2013, **3**, 4914-4916.

18. M. Raoa and X. Songb, *Electrochim Acta*, 2012, **65**, 228-233.
19. N. Jayaprakash, J. Shen, S. S. Moganty, A. Corona and L. A. Archer, *Angewandte Chemie International Edition*, 2011, **50**, 5904-5908.
20. X. Ji, K. T. Lee and L. F. Nazar, *Nature materials*, 2009, **8**, 500-506.
21. Y. S. Su and A. Manthiram, *Nat Commun*, 2012, **3**, 1166-1171.
22. Y. S. Su and A. Manthiram, *Chemical Communications*, 2012, **48**, 8817-8819.
23. X. Wang, Z. Wang and L. Chen, *Journal of Power Sources*, 2013, **242**, 65-69.
24. C. Zu, Y. S. Su, Y. Fu and A. Manthiram, *Physical chemistry chemical physics*, 2013, **15**, 2291-2297.
25. S. H. Chung and A. Manthiram, *Chemical Communications*, 2014, **50**, 4184-4187.
26. S. H. Chung and A. Manthiram, *ChemSusChem*, 2014, **7**, 1655-1661.
27. G. Ma, Z. Wen, J. Jin, M. Wu, X. Wu and J. Zhang, *Journal of Power Sources*, 2014, **267**, 542-546.
28. K. Zhang, Q. Li, L. Y. Zhang, J. Fang, J. Li, F. R. Qin, Z. A. Zhang and Y. Q. Lai, *Mater Lett*, 2014, **121**, 198-201.

Table

Table 1 Physical parameters of the CFs as interlayers

	Carbonization temperature / °C	Porosity / %	Electrolyte uptake / %	Electrical conductivity / S cm-1
CF-1	-	75	248	2.02 × 10-5
CF-2	300	69	299	2.05 × 10-5
CF-3	350	71	324	3.56 × 10-4
CF-4	400	85	381	4.57 × 10-4

Table 2 Summary of Li-S battery systems with an interlayer

Samples	Sulfur content	Sulfur loading (mg cm^{-2})	Specific capacity (mA h g^{-1})	Cycles	Ref.
microporous carbon paper	70%	-	1000 at 1 C	100	[21]
MWCNT interlayer	70%	-	962 at 0.2 C	50	[22]
rGO interlayer	85%	-	895 at 0.1 C	100	[23]
Toray carbon paper	60%	-	900 at 0.2 C	50	[24]
Carbonized Kimwipes	60%	1.1	1086 at 0.1 C	100	[25]
carbonized leaf	70%	1.3	1013 at 0.1C	100	[26]
PPy interlayer	65% (80% CMK-8)	1.5	846 at 0.2 C	200	[27]
pristine filter paper	70%	-	820 at 0.2 C	50	[28]
			560 at 1 C	50	
interlayer in this work	70%	2	858 at 0.1 C	100	
			677 at 1 C		

Figures Captions

Fig. 1 Schematic of Li-S battery with interlayer.

Fig. 2 Nitrogen adsorption/desorption isotherms (a) and pore size distribution plots (b) of CF-1, CF-2, CF-3, CF-4.

Fig. 3 SEM images of samples with or without heat treatment, (a) CF-1, (b) CF-2, (c) CF-3, (d) CF-4.

Fig.4 (a) Cycle performance of the Li-S cells with the CF-1, CF-2, CF-3, CF-4, and without the interlayer, at a rate of 0.1 C between 1.2 V and 2.8 V at room temperature. (b) Charge-discharge curves in different cycling numbers of the cell with CF-4 at a rate of 0.1 C.

Fig. 5 SEM images of CF-4 cross-section: (a) before cycle, (b) after 100 cycles. Digital photograph of the detachment Li-S cells: (c) without interlayer, (d) with CF-4. (e) The elemental mapping of sulfur of CF-4 after testing.

Fig. 6 (a) CV plots and EIS of the Li-S cell with (a) and (b) without interlayers. EIS plots of the Li-S cell with (c) and (d) without interlayers.

Fig. 7 The rate performance of the cell with and without interlayer.

Fig. 1

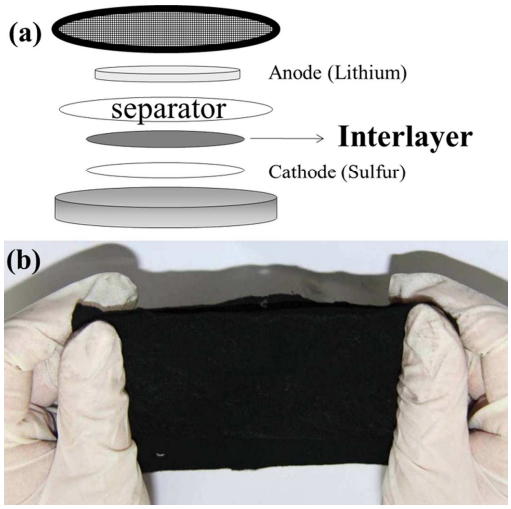

Fig. 1 Schematic of Li-S battery with interlayer.

Fig. 2

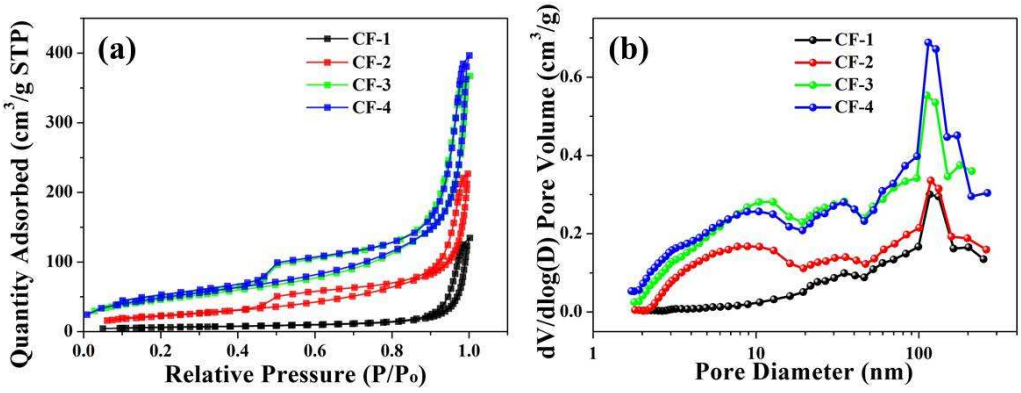

Fig. 2 Nitrogen adsorption/desorption isotherms (a) and pore size distribution plots (b) of CF-1, CF-2, CF-3, CF-4.

Fig. 3

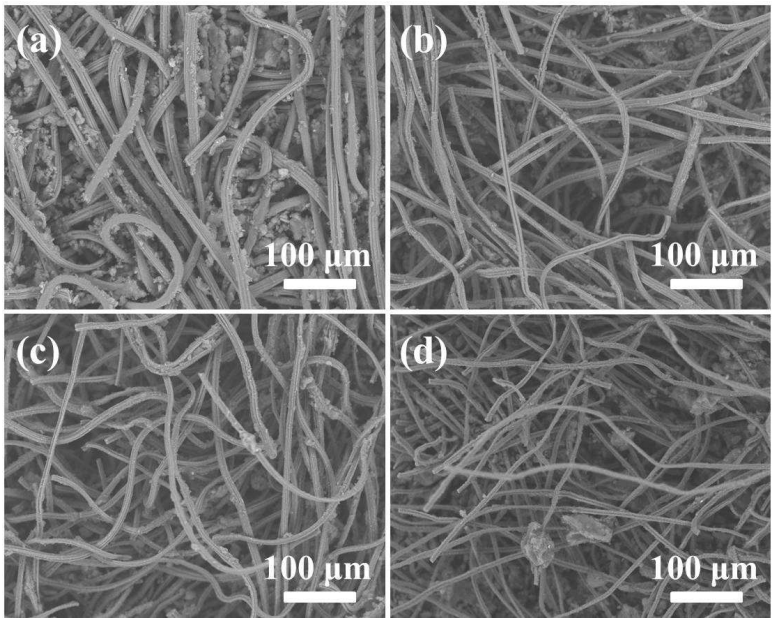

Fig. 3 SEM images of samples with or without heat treatment, (a) CF-1, (b) CF-2, (c) CF-3, (d) CF-4.

Fig. 4

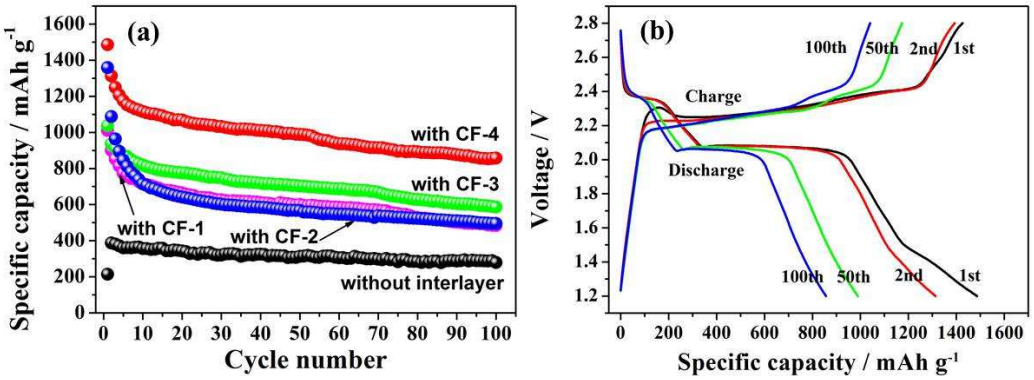

Fig. 4 (a) Cycle performance of the Li-S cells with the CF-1, CF-2, CF-3, CF-4, and without the interlayer, at a rate of 0.1 C between 1.2 V and 2.8 V at room temperature. (b) Charge-discharge curves in different cycling numbers of the cell with CF-4 at a rate of 0.1 C.

Fig. 5

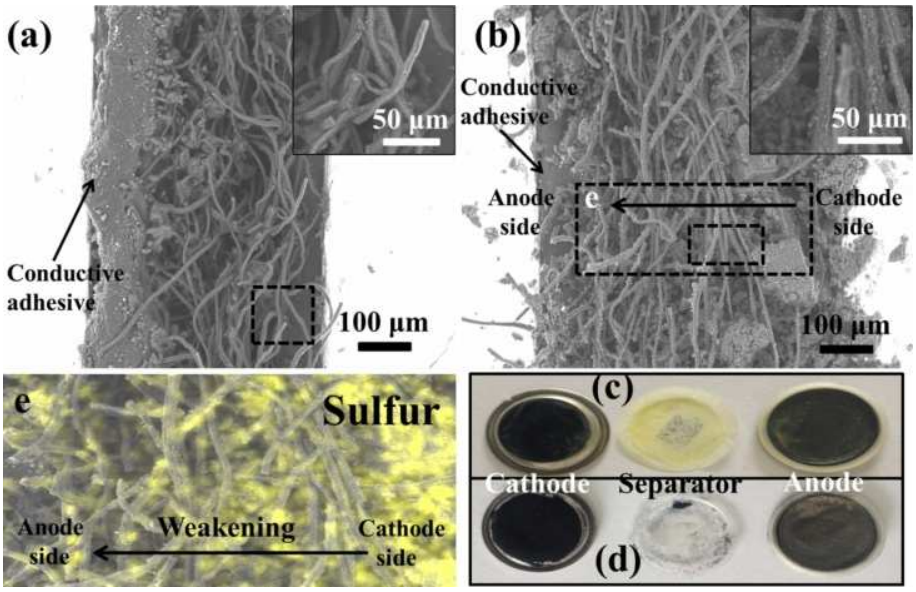

Fig. 5 SEM images of CF-4 cross-section: (a) before cycle, (b) after 100 cycles. Digital photograph of the detachment Li-S cells: (c) without interlayer, (d) with CF-4. (e) The elemental mapping of sulfur of CF-4 after testing.

Fig. 6

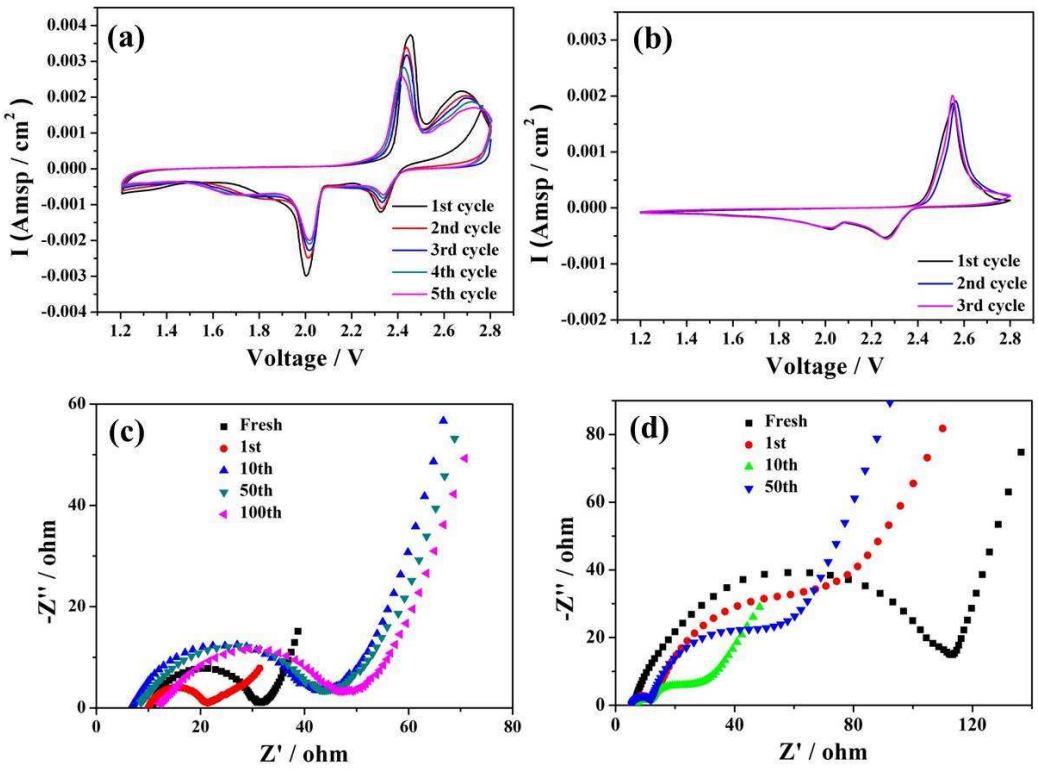

Fig. 6 CV plots and EIS of the Li-S cell with (a) and without (b) CF-4 interlayer. EIS plots of the Li-S cell with (c) and (d) without CF-4 interlayer.

Fig. 7

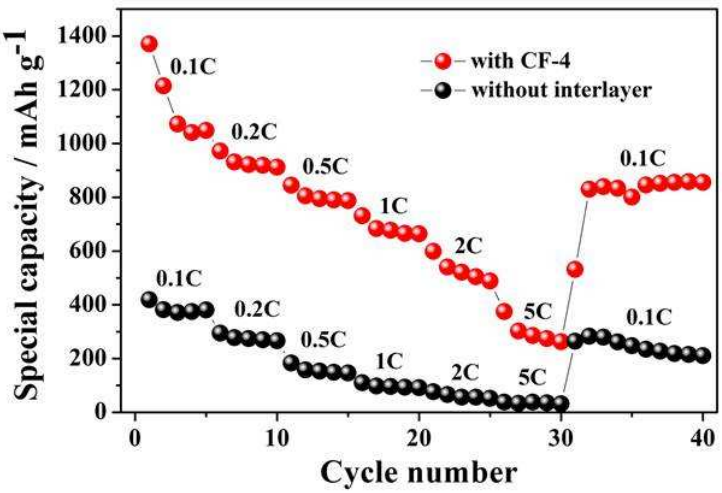

Fig. 7 The rate performance of the cell with and without interlayer.

Graphic abstract

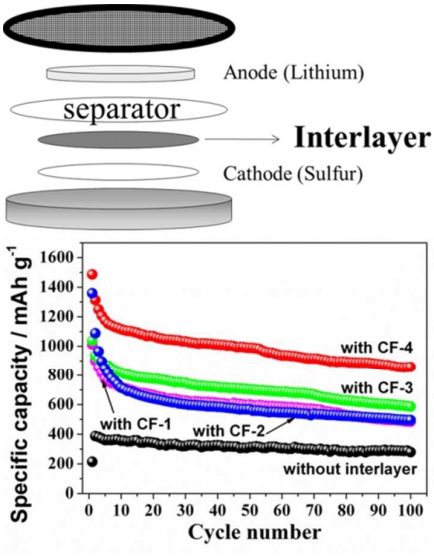

Carbonized non-woven fabrics film (CF) was used as adsorbing interlayer between the sulfur cathode electrode and the separator for high performance Li-S batteries with long term cycling stabilities, and a reversible capacity of 858 mA h g^{-1} was maintained after 100 cycles at rate of 0.1 C.